Science of the Total Environment 731 (2020) 138955

Contents lists available at ScienceDirect

Science of the Total Environment

journal homepage: www.elsevier.com/locate/scitotenv

Are there environmental or agricultural benefits in using forest residue biochar in boreal agricultural clay soil?

Helena Soinne [a,*], Riikka Keskinen [b], Jaakko Heikkinen [b], Jari Hyväluoma [c], Risto Uusitalo [b], Krista Peltoniemi [a], Sannakajsa Velmala [a], Taina Pennanen [a], Hannu Fritze [a], Janne Kaseva [b], Markus Hannula [d], Kimmo Rasa [b]

[a] Natural Resources Institute Finland, Latokartanonkaari 9, FI-00790 Helsinki, Finland
[b] Natural Resources Institute Finland, Tietotie 4, FI-31600 Jokioinen, Finland
[c] HAMK University of Applied Sciences, Mustialantie 105, FI-31310 Mustiala, Finland
[d] BioMediTech Faculty of Medicine and Health Technology, Tampere University, Tampere, Finland

HIGHLIGHTS

- Forest residue biochar significantly increased carbon stored in soil.
- Biochar amendment was not effective in reducing leaching of nutrients.
- Biochar did not change the clay soil water retention properties.
- Soil bacterial or fungal communities were not changed.
- A high biochar dose did not induce such positive impacts that would benefit farmers.

GRAPHICAL ABSTRACT

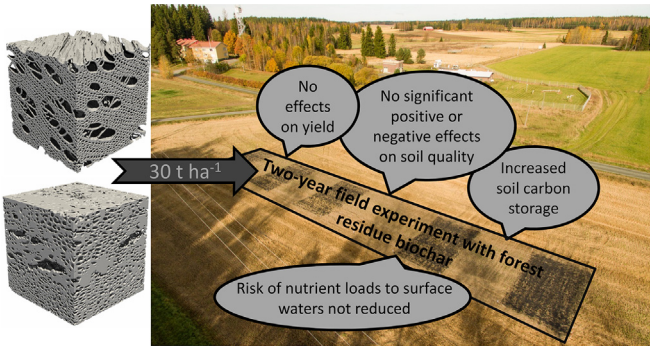

ARTICLE INFO

Article history:
Received 27 February 2020
Received in revised form 22 April 2020
Accepted 22 April 2020
Available online 28 April 2020

Editor: Fang Wang

Keywords:
Biochar
Carbon sequestration
Soil quality
Soil productivity
Nutrient leaching
Microbial community

ABSTRACT

Short-term agronomic and environmental benefits are fundamental factors in encouraging farmers to use biochar on a broad scale. The short-term impacts of forest residue biochar (BC) on the productivity and carbon (C) storage of arable boreal clay soil were studied in a field experiment. In addition, rain simulations and aggregate stability tests were carried out to investigate the potential of BC to reduce nutrient export to surface waters. A BC addition of 30 t ha^{-1} increased soil test phosphorus and decreased bulk density in the surface soil but did not significantly change pH or water retention properties, and most importantly, did not increase the yield. There were no changes in the bacterial or fungal communities, or biomasses. Soil basal respiration was higher in BC-amended plots in the spring, but no differences in respiration rates were detected in the fall two years after the application. Rain simulation experiments did not support the use of BC in reducing erosion or the export of nutrients from the field. Of the C added, on average 80% was discovered in the 0–45 cm soil layer one year after the application. Amendment of boreal clay soil with a high rate of BC characterized by a moderately alkaline pH, low surface functionalities, and a recalcitrant nature, did not induce such positive impacts that would unambiguously motivate farmers to invest in BC. BC use seems unviable from the farmer's perspective but could play a role in climate change mitigation, as it will likely serve as long-term C storage.

* Corresponding author.
E-mail address: helena.soinne@luke.fi (H. Soinne).

https://doi.org/10.1016/j.scitotenv.2020.138955

1. Introduction

Various environmental and agronomic benefits are pursued by adding biochar (organic biomass carbonized under low or no oxygen conditions) to agricultural soils (Sohi et al., 2010; Atkinson et al., 2010). On a global scale, the option of mitigating climate change by sequestering atmospheric carbon dioxide (CO_2) to fairly stable biochar carbon (C) offers major potential (Brassard et al., 2016; Lehmann, 2007; Matovic, 2011; Smith, 2016; Woolf et al., 2010). Compared to uncharred biomass, biochar C mineralizes 10 to 100 times more slowly (Lehmann et al., 2009). Consequently, biochar addition can lead to increased soil C stocks for centuries (Wang et al., 2016). Other potential biochar amendment-induced environmental advantages include improved soil aggregate stability (Lu et al., 2014; Soinne et al., 2014) and increased nutrient retention capacity (Saarnio et al., 2018; Borchard et al., 2012; Laird et al., 2010), both of which decrease the risk of erosion and off-site nutrient transport (Le Bissonnais, 1996; Sollins et al., 1988).

To attract farmers to invest in biochar, profits arising from the biochar treatment are required. The impacts of biochar amendments in soil have been extensively reviewed in the literature (Atkinson et al., 2010; Kavitha et al., 2018; Lehmann et al., 2011; Palansooriya et al., 2019; Sohi et al., 2010; Yu et al., 2019; Verheijen et al., 2009). Crop yield increase resulting from applied biochar can be achieved due to increased soil pH (Vaccari et al., 2011; Van Zwieten et al., 2010), improved nutrient use efficiency (Chan et al., 2008), and enhanced soil hydraulic properties (Abel et al., 2013; Laird et al., 2010). However, although the mean effect of biochar amendments on crop yields seems positive (Jeffery et al., 2011), the effect on yield in several experiments has been insignificant or even negative (Borchard et al., 2012, 2014; Jeffery et al., 2011; Tammeorg et al., 2014a; Tammeorg et al., 2014b Nelissen et al., 2015). In a recent global-scale meta-analysis by Jeffery et al. (2017), biochar was shown to stimulate yields in the tropics, probably through liming and fertilization effects, but not in the usually more fertile soils of temperate latitudes. In general, the highest positive agronomic responses can be expected from acid, coarse, and nutrient-poor soils (Liu et al., 2013; Jeffery et al., 2017). Negative impacts of biochar application may occur due to the reduced availability of nutrients e.g. by over-liming or N immobilization (Jeffery et al., 2017; Spokas et al., 2012). In soils with elevated P concentrations, biochar-induced increase in P availability may accelerate the risk of P loss (Saarnio et al., 2018). Furthermore, biochar application has potential of encasing soil microbial activity and diversity by providing favorable microbial habitats and substrates for their metabolic activities (Palansooriya et al., 2019), but on the other hand, biochar may contain toxic compounds that have negative impacts on soil microbes (Gomez et al., 2014). Therefore, both the direct positive and negative effects of biochar on soil biota and subsequent impacts on soil processes need to be considered (Chintala et al., 2014; Lehmann et al., 2011).

Besides climatic and soil conditions, the characteristics of the biochar itself govern potential responses in soil (Novak et al., 2009). The process conditions of the thermal treatment influence the biochar properties (e.g. C content, stability, internal porosity, pH, and surface area and surface activity) to a great extent, but the type of feedstock, namely its C and ash content and composition, also have a major effect on the char quality (Ronsse et al., 2013; Sun et al., 2014; Windeatt et al., 2014; Lee et al., 2013; Zhao et al., 2013). An extensive forestry sector in the boreal climate zone results in a large amount of potential biochar raw material in the form of forest residue (e.g. small trees, branches, and stumps). After clear cutting and thinning, wood material unsuitable for industrial use is either left on site or harvested as bioenergy. The annual gross potential of forest residues in Finland and Sweden is >100 million solid m^3, while the realistically achievable amount is around 40 million solid m^3 (Routa et al., 2013). From the perspective of C sequestration, forest residue decomposes relatively quickly when left on site. Depending on the diameter of branches, after 100 years of decomposition only 2–16% of the initial branch biomass remains (Repo et al., 2011). When incinerated as bioenergy, the C release into the atmosphere is immediate. Thus, the C sequestration potential of forest residue biochar is remarkable. However, the properties and performance of forest residue-based biochar in the agricultural context need to be verified to motivate farmers to adopt such actions.

In this study, a field experiment was established to assess the impacts of forest residue biochar (BC) on a boreal low-productive clay soil. We aimed to find out whether short-term gains in productivity or non-yield-related factors can be achieved by BC to justify recommending the treatment and prompt the interest of farmers and relevant authorities in wider BC use. The effects of BC addition on plant growth, soil structure, fertility (pH and available nutrient concentrations), moisture characteristics, fungal and bacterial biomass and communities, gross microbiological activity, and soil C storage were examined over two consecutive growing seasons after the BC application. In addition, the potential of BC to reduce nutrient export to surface water was investigated under simulated rainfall.

2. Material and methods

2.1. Forest residue biochar

BC used in the experiment was produced by a continuously operated pilot-scale mobile pyrolysis unit (Raussin metalli Ky, Sippola, Finland) in the fall of 2016. The raw material used was chipped forest residue from thinnings and/or clear cuttings containing stems, branches, and small wood, but not stumps. The maximum temperature the material was heated to was about 450 °C. The produced BC was mixed and milled using a large-scale hammer mill, and thereafter packed into 5 large bags of equal weight. After homogenization, the BC dry matter content was 59%.

BC was analyzed for pH (H_2O) and electrical conductivity (EC) in 1:5 solid-to-water paste (Table 1). Oxygen (O) content was calculated as the difference between the initial dry mass and sum of ash (815 °C), C, nitrogen (N), and hydrogen (H) contents determined by Vario MAX CHN Elementar-Analysator. Other elements listed in Table 1 were analyzed after aqua regia extraction with ICP-OES. Exchangeable cations were extracted with neutral ammonium acetate (1 M CH_3COONH_4, pH 7.0) and the concentrations of Ca, Mg, K, and Na were analyzed from this solution by an ICP-OES (Perkin Elmer Optima 8300). The cation exchange capacity (CEC) was determined as adsorbed NH_4-N exchanged out by 2M KCl solution. Surface acidic functionalities were

Table 1
Chemical characteristics of the forest residue biochar (BC).

Variable (unit)	Value	Variable (unit)	Value	Variable (unit)	Value	Variable (unit)	Value
pH	8.23	K (g kg^{-1})	3.7	Cu (mg kg^{-1})	10	CEC (cmol kg^{-1})	12
EC (μS cm^{-1})	174	Fe (g kg^{-1})	3.0	Ni (mg kg^{-1})	2.7	Ca_{exc} (g kg^{-1})	4.2
Ash, 815 °C (%)	6.3	Mg (g kg^{-1})	1.2	Cr (mg kg^{-1})	2.5	K_{exc} (g kg^{-1})	2.10
C (%)	80	P (g kg^{-1})	0.99	Co (mg kg^{-1})	0.96	Mg_{exc} (g kg^{-1})	0.20
H (%)	3.1	Al (g kg^{-1})	0.62	Cd (mg kg^{-1})	0.89	Na_{exc} (mg kg^{-1})	20
N (%)	0.8	Mn (mg kg^{-1})	310	As (mg kg^{-1})	0.32	Carboxyls (meq g^{-1})	0.03
O (%)	9.8	Zn (mg kg^{-1})	247	Pb (mg kg^{-1})	<3.0	Lactones (meq g^{-1})	0.09
Ca (g kg^{-1})	9.6	S (mg kg^{-1})	143	Mo (mg kg^{-1})	<2.0	Phenols (meq g^{-1})	0.16

determined by Boehm titration (Boehm et al., 1964) according to Kim et al. (2012)

2.2. X-ray microtomography

The internal structure of four randomly selected BC particles was imaged with x-ray computed microtomography. The sample size was c. 1 mm. Imaging of the samples was performed with a Zeiss Xradia MicroXCT-400 (Zeiss, Pleasanton, CA, USA) device. In total, 1600 full 360° projections were acquired for each sample. The exposure time for each projection was 3 s, and the source voltage and current were 40 kV and 250 μA respectively. A 20× objective was used with binning 2, resulting in a pixel size of 1.132 μm. No filters were used in the imaging. The image stacks were reconstructed with the filtered back projection algorithm using Zeiss XMReconstructor software.

For quantitative analysis of the micrometer-scale pore structure, the original grayscale images were segmented into a binary representation of pore and solid phases. Image processing was performed in several steps. Grayscale images were denoised by variance-weighted (VaWe) mean filtering (Gonzalez and Woods, 2001). The denoised images were segmented into pores and solids, using the segmentation method developed by Sauvola and Pietikäinen (2000). The segmented binary images were further filtered with a majority filter, and finally, all isolated solid objects with a volume <1000 voxels were removed from the images. The binary image thus obtained was used in the image analysis.

Image analysis was used to determine the porosity and pore-size distribution of the imaged BC samples. The pore size distributions of the samples were determined using an approach based on mathematical morphology (Horgan, 1998) by successive application of morphological opening with an increasing structuring element diameter (e.g. Hilpert et al., 2003). The pore size defined by morphological opening is closely related to the stationary distribution of water in pore space. This method is therefore suitable for the present purpose, because it relates to the pore sizes used in the interpretation of soil moisture characteristic curves.

2.3. Field study and soil properties

The BC field experiment was conducted at the Natural Resources Institute Finland (Luke) in Jokioinen, southwestern Finland on a clay soil field. Clay soils of the area have typically been classified into (Vertic Luvic) Stagnosols (Lilja et al., 2017). Like the majority of the fields in Finland, the experimental field was artificially drained. The previous yield data and practical experience suggested relatively poor growing conditions for the chosen experimental area. In the top 20 cm layer, clay, silt, and sand content was 64%, 21%, and 15% respectively. C content (dry combustion, Leco TruMac CN analyzer) was on average 5.1% in the 0–10 cm soil layer and 4.6% in the 10–20 cm soil layer. Soil test phosphorus (STP) and other nutrients extracted with acid ammonium acetate (AAAc, pH 4.65; Vuorinen and Mäkitie, 1955) were at least good according to the Finnish guidelines for the status of a soil test.

The study area comprised 10 plots of 60 m^2 (6 × 10 m) arranged in five blocks, for which the BC and control treatments were randomized (randomized block design). The BC application was done in the autumn 2016 at the rate of 30 Mg dry matter ha^{-1}. Spreading of BC was done manually to ensure an even application over the plots. Immediately after the spreading of BC (October 2016), all plots were cultivated to approximately 10–12 cm depth, using the Kongskilde cultivator. In 2017 and 2018, the field was sown for oats and was fertilized (N 90 kg ha^{-1}, P 10 kg ha^{-1}) according to the Finnish guidelines, taking into account the results of the national soil test procedure.

In 2017, the thermal growing season (daily mean temperatures consistently above 5 °C) started on May 1 and ended on October 18. The field was sown with oats on May 19 and harvested on September 28. The temperature sum of 2017 was 1200 °C and below the long-term average of 1300 °C (1981–2010, statistics from the Finnish Meteorological Institute), whereas the amount of rain during the growing season (c. 400 mm) exceeded the long-term average (350 mm). In 2018, the growing season started already on April 14. After a very dry spring, oats were sown on May 31 and harvesting was done on September 12. The temperature sum of 2018 was 1700 °C and above the long-term average, whereas the amount of rain during the growing season (c. 300 mm) was below average. The mean daily temperature during 2017 and 2018, and the rain sum of both years, is presented in the Supplementary material (Supplementary material 1). Grain yields were calculated using the mass and moisture content of grains harvested from a 20 m^2 area in each plot. The element contents of seeds were analyzed after HNO_3 digestion (ICP-OES, Perkin Elmer Optima 8300) and N content was analyzed by the Kjeldahl method (Foss Kjeltec™ 8400). The schedule of soil and plant sampling and subsequent analyses are summarized in Table 2.

2.4. Soil analyses

Before sowing in 2018, soil samples for an analysis of bulk density and total C (TC) and nitrogen (TN) were taken from each plot in four different layers (0–10, 10–20, 20–30, and 30–45 cm) with a 45.2 mm diameter auger. These samples of known volume were dried at 40 °C and weighed for the bulk density measurement. Thereafter, the samples were ground and analyzed for C and N (Leco TruMac CN). Calculation of soil C stock in the soil profile was based on the measured bulk density and C content.

In the fall of 2018 after the harvest, composite soil samples from each plot were collected from 0–10 and 10–20 cm layers for analysis of pH and EC (1:5 H_2O). In addition, these samples were analyzed for soil test phosphorus (STP) and Ca, Mg, K, Na, and S in accordance with the Finnish national soil test procedure (Acid ammonium acetate, AAAc, extraction, Vuorinen and Mäkitie, 1955). Mehlich3 (Meh3) extraction (Mehlich, 1984) was carried out to analyze P (colorimetric method), Al, and Fe (ICP-OES).

2.5. Soil moisture characteristics

In the fall of 2018 after the harvest, undisturbed soil samples were taken in moist soil conditions. First, a 2.5 cm layer of surface soil was removed. A 200 cm^3 steel cylinder (diameter 7 cm) was then gently pressed to a depth of 2.5–7.5 cm (i.e. within the mixing depth of BC).

Table 2
Samples taken from the forest residue biochar (BC) field experiment and analyzes performed during the study period 2017–2018.

Sampling time	Measure, sampling purpose
Fall 2016, after harvest	BC application
Spring 2017, before sowing	Monoliths for rainfall simulation
Fall 2017, at the time of harvest	Yield mass and nutrient contents in the seeds
Spring 2018, before sowing	Monoliths for rainfall simulation Bulk density and TC, TN down to 45 cm Samples for the aggregate stability test (0–5 cm) Samples for basal respiration and DNA extraction (0–10 cm)
Fall 2018, before harvest	Samples for basal respiration and DNA extraction (0–10 cm) Samples for microbial biomass and PLFA (0–10 cm)
Fall 2018, at the time of harvest	Yield mass and nutrient contents of the seeds
Fall 2018, after harvest	Samples for acid ammonium acetate extraction (AAAc) (0–10 and 10–20 cm) Samples for pH, EC (0–10 and 10–20 cm) Samples for Mehlich3-P, —Al, and —Fe (0–10 and 10–20 cm) Soil cores for pF-curve (2.5 cm–7.5 cm) Steady-state infiltration rates

The cylinders were excavated from the soil, closed with plastic lids, and stored at +4 °C in closed plastic bags to avoid drying. Five replicate samples were taken from each of the 10 plots. Samples were saturated with water for two weeks, and a pressure chamber approach was thereafter used to determine the soil moisture characteristic curve in suction pressure steps of 3.2, 5.0, 10.0, 15.8, 25.1, 39.8, 100, and 316 kPa. A vapor pressure equilibrium approach with saturated ammonium oxalate and sodium chloride solution was used to determine moisture content at 1500 kPa (permanent wilting point) and 39,000 kPa. Shrinkage of the samples during the drying process was measured both vertically and horizontally in each of the suction pressure steps. The vertical shrinkage was measured at five locations per sample using a Vernier caliper, and the horizontal shrinkage from four locations using a feeler gauge.

The effect of BC application on soil porosity was studied using the soil water characteristic data. The suction pressures were converted to approximate pore sizes using the Young-Laplace equation, and the water content of the samples were interpolated at 5 μm pore intervals using linear interpolation. Finally, the effect of BC on porosity was calculated as the difference between the pore size distribution of samples with BC and control. The calculation procedure is described in detail in Rasa et al. (2018).

2.6. Tension infiltrometry

The steady-state infiltration rates of water into the soil were determined in October 2018 with tension infiltrometers manufactured by Soil Measurement Systems LLC (Huntington Beach, CA, USA). The used devices consist of a porous disk (diameter 20 cm) which is separated from the water reservoir and bubble towers. At each measurement site, the vegetation was first cut to soil level, and the soil surface was then gently leveled and smoothed. A thin layer of moist fine sand was used to ensure good contact between the infiltration disk and the soil surface. Measurements were performed at supply pressure heads of −6, −3, and −1 cm in an ascending sequence. The measurements were continued until a steady-state infiltration was reached. The hydraulic conductivity at each supply pressure was calculated using the method described by Ankeny et al. (1991), which is based on Wooding's theory of unconfined three-dimensional infiltration (Wooding, 1968).

2.7. Rainfall simulation and aggregate stability test

Undisturbed soil monoliths (height 40 cm, diameter 30 cm) for rainfall simulation (Uusitalo et al., 2012) were collected by a tractor-driven auger (see Persson and Bergström, 1991) from each plot on May 3, 2017 and May 22, 2018. The samples were transported to the laboratory and stored at about +6 °C in the dark for <3 weeks.

Before rainfall simulation tests, the bottom of the samples was prepared for natural plains of cleavage, and the voids were filled with coarse quartz sand and finally secured in sample holders. The samples were slowly saturated with water one day from the bottom to the level of soil surface. The water level was maintained over two days and then allowed to drain overnight. A stationary drop-former was used in the rainfall simulation tests (Uusitalo and Aura, 2005). The rainfall intensity was adjusted to 5 mm h^{-1} (deionized water with kinetic energy about 80 J m^{-2} h^{-1}), which is typical intensity for rain in South-West Finland. The samples were subjected to 5 h of rainfall in two subsequent days. Water samples were collected during these rainfall periods and in addition, the percolation water drained overnight between days 1 and 2 was collected. Consequently, four water samples per each monolith were collected: (i) water draining overnight after the initial saturation, (ii) percolation water obtained during the first rainfall event, (iii) water draining overnight after the first day of rainfall simulations, and (iv) percolation water obtained during the second rainfall event. Each of these water samples were analyzed separately, but the results are presented as their mean values.

Turbidity of each water sample was measured immediately (2100AN IS Turbidimeter, Hach Company) followed by EC and pH analyses. A part of the water sample was filtered through 0.2 μm Nuclepore (Whatman) membrane and both filtered and unfiltered fractions were frozen and stored at −18 °C until further analyses. The filtered subsamples were analyzed for dissolved molybdate-reactive phosphorus (DRP), NO_3-N and NH_4-N. Following autoclave digestion with peroxodisulphate and sulphuric acid, the unfiltered samples were analyzed for total P and N concentrations. The P and N species were determined using a continuous flow injection analyzer (LaChat autoanalyzer). Before analyses for dissolved organic carbon (DOC) with a Shimadzu TOC analyzer, water samples were passed through Whatman GF/C glass filters.

In the spring 2018, soil surface samples (0–5 cm) were taken for aggregate stability tests from each plot at 3 different locations. The samples were kept at sampling moisture and dry sieved to retain an aggregate fraction of 2–5 mm. The sieved aggregates were air-dried and 4 g (dry matter) from each sample was subjected to wet sieving (Heikkinen et al., 2019) with an Eijkelkamp 08.13 apparatus equipped with 0.25-mm mesh size sieves. The aggregates placed on the sieves were pre-moistened for 15 min in cans containing 100 ml of deionized water. The pre-moistening was followed by a 3 min up-and-down run with the wet sieving apparatus. Water-stable aggregates remaining on the sieves were oven-dried (110 °C) and weighed. The proportion of water-stable aggregates (WSA%) was calculated by dividing the weight of the material on the sieves by the total weight of the initial material. The suspension containing soil material that passed through the sieves was transferred to a 100-ml container and left to settle for 21 h. Samples for turbidity measurements were pipetted from the surface of the container, and turbidity (in nephelometric turbidity units, NTU) was determined using a HACH 2100AN IS turbidimeter (Hach Company). The turbidity values were divided by the dry mass of the aggregates taken for the analysis.

2.8. Basal respiration, DNA extraction, bioinformatics, qPCR, and amplicon sequencing

In 2018, samples were collected for microbiological analyses. Samples from the surface soil (0–10 cm) of each plot (composite samples comprised of ten subsamples) were collected before sowing in the spring and after the harvest in the fall. After the sampling and prior to the analyses, samples were stored cold (+4 °C). Prior to respiration measurements, the soil samples were kept at 14 °C for two days. The basal respiration rate was determined from fresh soil (20 ml), as the amount of CO_2 evolved during 24 h incubation and was measured as described by Pietikäinen and Fritze (1995).

The DNA of all control and BC-amended plots (n = 5) in both the spring and fall samples was extracted with a NucleoSpin soil kit (Macherey Nagel, Germany) in line with the manufacturer's protocol. For amplicon sequencing, the replicate samples of the DNA extractions from the fall sampling were combined to form one control and one BC-amended sample. These DNA samples were delivered for sequencing at Tartu University's Institute of Genomics. For bacteria, targeting the 16S V4 region of the 16S SSU rRNA gene was amplified in a two-step PCR, using the 16S rRNA 515F and 806R primers (Caporaso et al., 2011, 2012), and for fungi targeting, using an internal transcribed spacer 2 (ITS2) region with ITS4 (White et al., 1990) and gITS7 (Ihrmark et al., 2012) primers with an 8 bp dual index for 24 cycles. The final PCR fragments were run as paired-end 2 × 300 bp with MiSeq platform (Illumina), using MiSeq v3 kit producing about 20–25 M reads per flow cell. Quantitative PCR for the fungal ITS region and bacterial and archaeal 16S rRNA gene was conducted as described in Peltoniemi et al. (2015) for all samples separately.

Sequence assembly, quality filtering, removal of artifacts, primer-dimers and primers from raw 16S rRNA and ITS2 sequence reads, along with clustering and taxonomical annotations, were conducted

with a PipeCraft 1.0 pipeline (Anslan et al., 2017). PipeCraft utilizes several implemented tools of e.g. mothur v1.36.1 (Schloss et al., 2009), vsearch v1.11.1, and CD-HIT v4.6 (Fu et al., 2012), which were used in pre-processing, assembling, chimera filtering, and clustering steps. Raw sequence reads were processed according to the manual, with slight modifications for demultiplexed sequence data. Briefly, assembly of paired-end reads and initial quality filtering was conducted with vsearch (v1.11.1; github.com/torognes/vsearch; Rognes et al., 2016) according to the following parameters: minimum overlap 15; max differences 99; minimum length 150 bp; e_max 1; max ambiguous 0 and trunc qual 20 for fungi and 10 for bacteria. On average, 37% of the raw reads were filtered out after the assembly. Chimera filtering was performed for the reoriented reads using vsearch de novo filtering with parameters: annotation 0.97 and abskew 2; and for ITS both reference-based filtering was used with Unite ITS2 ref. v7.1 as a database. Primers and primer artifacts were also filtered out from sequences at this step. In addition, fungal ITS2 region was extracted from reads with ITSx (Bengtsson-Palme et al., 2013). In the next step, sequence reads were clustered and OTU table created with CD-hit with parameters: threshold 0.97; and min size 2. In the last step, bacterial OTUs were taxonomically annotated by searching for representative sequences with BLAST using the reference 16S rRNA (SILVA_123_SSURef_Nr99_tax_silva.fasta) obtained from SILVA (Quast et al., 2012; Yilmaz et al., 2014). For the fungi, the ITS2 database (sh_genral_release_dynamic_01.12.2018.fasta) from UNITE (Nilsson et al., 2018) was used. After the first quality filtering steps, raw sequence data for bacteria consisted of 40,013 reads clustering in 1967 OTUs. For fungi, 47,366 reads clustered in 691 OTUs.

Second quality filtering was done based on the results of the alignments: We filtered out bacterial and fungal OTUs that had an e-value higher than e-25, query coverage <90%, and identity <90% with the database match. OTUs with an affiliation other than bacteria or fungi, as well as singleton OTUs and reads with a relative proportion below 0.0001%, were removed from the data. Furthermore, fungal OTUs referring to exactly the same species hypothesis (Kõljalg et al., 2013) were consolidated. Bacterial OTUs were not consolidated. This resulted in 36,195 reads that were affiliated to 889 bacterial OTUs, and 41,259 fungal reads that were affiliated to 296 OTUs. The raw sequence data was deposited in the sequence read archive (SRA) of the NCBI/EMBL database, BioProject PRJNA599338, with the accession numbers SAMN13745490 and SAMN13745497.

2.9. Microbial community composition by PLFA analyses

Biomass and phospholipid fatty acid PLFA analyses were performed for samples taken in the fall after the harvest. Prior to the analyses, samples were stored cold (+4 °C). The phospholipid extraction and analysis of PLFAs were carried out as described by Frostegård et al. (1993). Briefly, 2.5 g of fresh soil was extracted with a chloroform:methanol:citrate buffer mixture (1:2:0.8) and lipids were thereafter separated into neutral lipids, glycolipids, and phospholipids on a silicic acid column. The phospholipids were subjected to mild alkaline methanolysis, and fatty acid methyl esters were detected with a gas chromatograph (GC) using a flame ionization detector and 50-m HP-5 capillary column (see GC-run configuration in Pennanen et al., 1999). In total, 43 different PLFAs were identified from each sample, and they were expressed as a mole percentage (mol % = area % of a single PLFA from the area sum of all identified PLFAs). All the identified PLFAs were used to calculate the total biomass indicator $PLFA_{tot}$.

The following PLFAs were considered to be predominantly of bacterial origin: i15:0; a15:0; 15:0; i16:0; 16:1ω9; 16:1ω7t; i17:0; a17:0; 17:0; cy17:0; 18:1ω7; and cy19:0. They were chosen as an index of bacterial biomass $PLFA_{bact}$ (Frostegård and Bååth, 1996). The amount of 18:2ω6 was used as an indicator of fungal biomass, $PLFA_{fung}$, because it is suggested to be mainly of fungal origin in soil (Federle, 1986) and is known to correlate well with the amount of ergosterol (Frostegård and Bååth, 1996).

2.10. Statistical analyses

The BC treatment induced differences in soil chemical properties and aggregate stability were tested with a one-way analysis of variance for randomized block design using BC treatment as a fixed effect. Turbidity values indicating colloid detachment during the wet sieving did not meet the requirements of analysis of variance (Shapiro-Wilk test for normality) and were analyzed with a nonparametric Wilcoxon rank-sum test. In the analyses of yields and nutrient content in the seeds measured in 2017 and 2018, as well as in microbiological properties that were measured twice during the growing season, a two-way analysis of variance was used with BC treatment and the sampling event as fixed effects. Pairwise comparisons between the control and BC treatment in each year were performed using Tukey's test. For the nutrient contents in the seeds that were not normally distributed, a nonparametric Wilcoxon rank-sum test was used.

The area% of each PLFA was used to analyze the variation in PLFA composition using principal components analysis (PCA) followed by Analysis of Variance (ANOVA) to test differences in PC scores and PLFA biomass values.

Statistical analyses of near-saturated hydraulic conductivity (K_{unsat}) and soil water holding capacity were based on a repeated measures design with two treatments (BC and control), three supply pressure heads (−6, −3, and, −1 cm) or eleven matric potentials respectively, and five replicates in blocks. Generalized linear mixed models (GLMM) with lognormal (with an identity link) and beta (with a logit link) distributions were used for K_{unsat} and soil water holding capacity respectively, with a treatment and suction pressure head or suction pressure point respectively, and their interaction as fixed effects. The effects of block and treatment within a block were used as random effects. Correlation between supply pressure heads or suction pressure points within treatment in a block was considered in using an unstructured and homogeneous autoregressive covariance structures respectively (Gbur et al., 2012).

In the rain simulation experiment, means of pH, nutrient concentration, and turbidity (NTU) in BC-amended and control soils in 2017 and 2018 were compared by GLMMs. Treatment and year, and their interaction, were used as fixed effects, and the block and the interaction of block and year as random effects. Correlation between years was taken into account using a heterogeneous or homogeneous compound symmetry covariance structure. The assumptions of gamma (with log link) and lognormal (with identity link) distributions were used for TP and turbidity respectively. Other dependent variables were assumed to be normally distributed.

All models were fitted by using the residual pseudo likelihood (TP and soil water holding capacity) or restricted maximum likelihood (others) estimation method. The degrees of freedom were calculated using the Kenward-Roger method (Kenward and Roger, 2009). The normality of residuals was checked using boxplot, and residuals were plotted against the fitted values. Westfall's (1997) method was used for pairwise comparisons of means, with a significance level of $\alpha = 0.05$. The analyses were performed using the GLIMMIX procedure of the SAS Enterprise Guide 7.15 (SAS Institute Inc., Cary, NC, USA).

3. Results

3.1. Yields and harvest quality

There were no differences in yield masses between the control and BC-treated plots. However, yields were significantly lower in the second and much dryer year (Supplementary material 2), but even then, oat growth did not benefit from the BC treatment.

The contents of major elements (N, K, P, S, Mg, Ca) in oat seeds were not affected by the BC amendment (Supplementary material 2). For elements in low contents (mg kg^{-1} and ug kg^{-1}), only Ni, Zn, and Mo showed differences between treatments. In the first harvest after the

BC addition in 2017, Mo and Zn were significantly higher in seeds grown on BC-treated soil. In the second harvest in 2018, the Ni content in oat seeds was significantly lower in BC-treated plots (Supplementary material 2).

3.2. Soil pH, EC, and available nutrients

Two years after the BC treatment, soil pH or EC did not differ between control and BC-treated plots (Table 3). In BC-treated plots, STP (acid ammonium acetate extractable P) was higher in the 0–10 cm soil layer than in the control plots, but no differences were detected in the 10–20 cm soil layer. A similar trend was seen in the soil P_{Meh3} for the surface soil, but the difference between the treatments was not significant ($p = 0.0814$). Of major cations, only soil test Ca was higher in BC-treated plots.

3.3. Bulk density, carbon, and nitrogen in soil profile

Bulk densities measured in the spring of 2018 were lower at the 0–10 cm soil surface layer of BC-treated plots ($p = 0.0113$), but no differences were detected in the 10–20 cm layer (Fig. 1). BC addition increased C content in the 0–10 cm layer ($p = 0.0051$), but below this, no clear differences were detected. The BC treatment showed no effect on soil N content in the two different layers. When measured to a fixed soil depth (45 cm), the stock of C in BC-treated plots (163 Mg ha^{-1}) was higher ($p = 0.0167$) than in control plots (144 Mg ha^{-1}), but the stock of N did not differ between the treatments, being 11.4 and 11.1 Mg ha^{-1} in BC and control plots respectively.

3.4. Soil moisture characteristics and infiltration

Compared to the control, the BC amendment tended to increase soil water holding capacity up to the suction pressure of 25 kPa (Fig. 2). The lower the suction pressure, the greater the difference tended to be. The differences in soil water holding capacity between the control and samples with BC were not, however, statistically significant at $p < 0.05$ level ($p = 0.07$–0.88), but at the $p < 0.1$ level a significant difference was found at near-saturated conditions (0.25 kPa). The application of BC especially increased the share of pores smaller than a 10-μm diameter (Fig. 2). Another peak was found in pore size range of around 25–30 μm. The near-saturated hydraulic conductivity was not affected by a BC addition at any supply pressure head (−1, −3, and, −6 cm $p = 0.3745$, $p = 0.2694$, and $p = 0.1212$ respectively, Fig. 3).

3.5. Porosity of forest residue biochar, X-ray microtomography

Visual inspection of 3D images showed, that three of the BC samples had a pore structure typical of deciduous trees, while the structure of one sample was clearly different and was probably from a coniferous tree (Supplementary material 3). Porosity of the samples varied such that the clearly different sample had the lowest porosity (0.37), while for the three other samples, porosities ranged between 0.45 and 0.49. The pore size distributions of the samples are shown in Fig. 4. Three samples had a bimodal pore size distribution, and one sample had unimodal distribution. In the samples with bimodal distribution, the pore diameter of the first maxima (tracheids) was in the range 5–10 μm. The size of the pores leading to the second maxima (vessels) differed, being c. 30–35 μm in sample S1 (cf. Fig. 4),

Table 3
Soil pH and electrical conductivity (EC, μS cm^{-1}), Mehlich3-P, -Al, and -Fe (Meh3, mg kg^{-1} soil) and AAAc (pH 4.65) extractable P and cations (Ca, Mg and K) (mg kg^{-1} soil) at two depths (0–10 cm and 10–20 cm) measured two years after the BC treatment. CI = 95% confidence interval. Statistically significant differences were tested separately for both layers.

	0–10 cm					10–20 cm				
	Control	CI	BC	CI	*p*	Control	CI	BC	CI	*p*
pH	5.7	[5.6, 5.8]	5.8	[5.7, 5.9]	0.337	5.7	[5.7, 5.8]	5.8	[5.7, 5.8]	0.683
EC	99	[89, 109]	97	[87, 107]	0.798	96	[88, 104]	96	[88, 105]	0.964
Al_{Meh3}	1719	[1690, 1747]	1720	[1692, 1749]	0.908	1631	[1595, 1666]	1638	[1602, 1673]	0.726
Fe_{Meh3}	509	[481, 537]	525	[497, 553]	0.318	479	[472, 486]	479	[472, 486]	0.917
P_{Meh3}	57	[46, 68]	70	[58, 81]	0.092	40	[37, 43]	37	[34, 40]	0.173
P_{AAAc}	11.9	[10.8, 12.9]	13.5	[12.5, 14.6]	0.039	10.0	[9.2, 10.8]	9.6	[8.8, 10.4]	0.409
Ca_{AAAc}	2491	[2427, 2555]	2608	[2544, 2672]	0.023	2551	[2482, 2620]	2597	[2529, 2666]	0.257
Mg_{AAAc}	706	[677, 736]	711	[681, 740]	0.784	744	[707, 782]	739	[702, 776]	0.783
K_{AAAc}	787	[737, 836]	849	[800, 899]	0.069	738	[701, 775]	783	[746, 819]	0.075

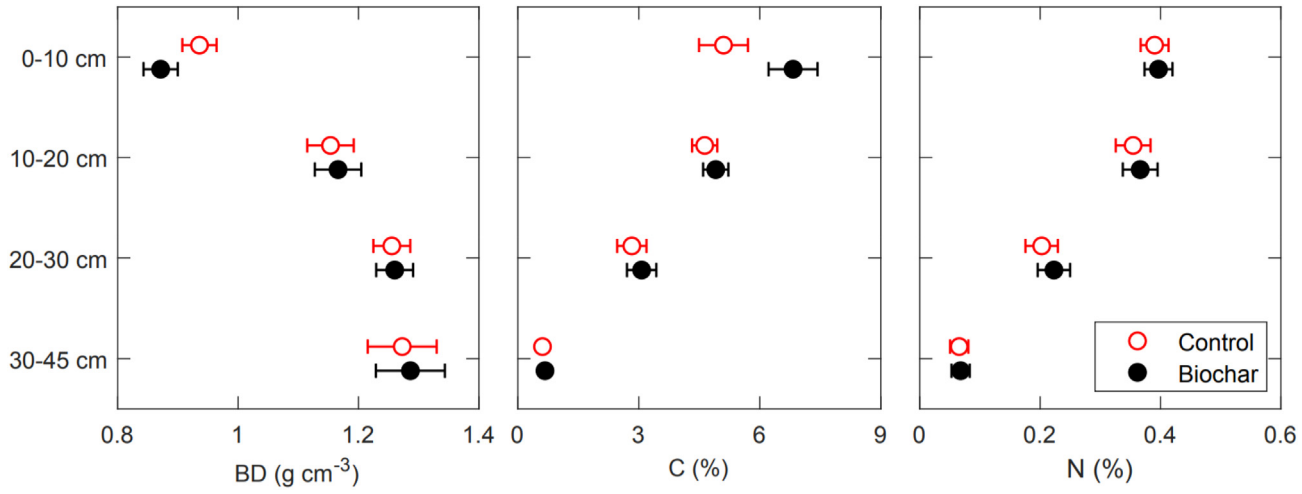

Fig. 1. Bulk densities (BD, g cm^{-3}), C% and N% in control and in BC-treated plots two years after the BC application at different depths (mean and 95% confidence intervals). Only BD and C% at the 0–10 cm layer differed significantly between the treatments.

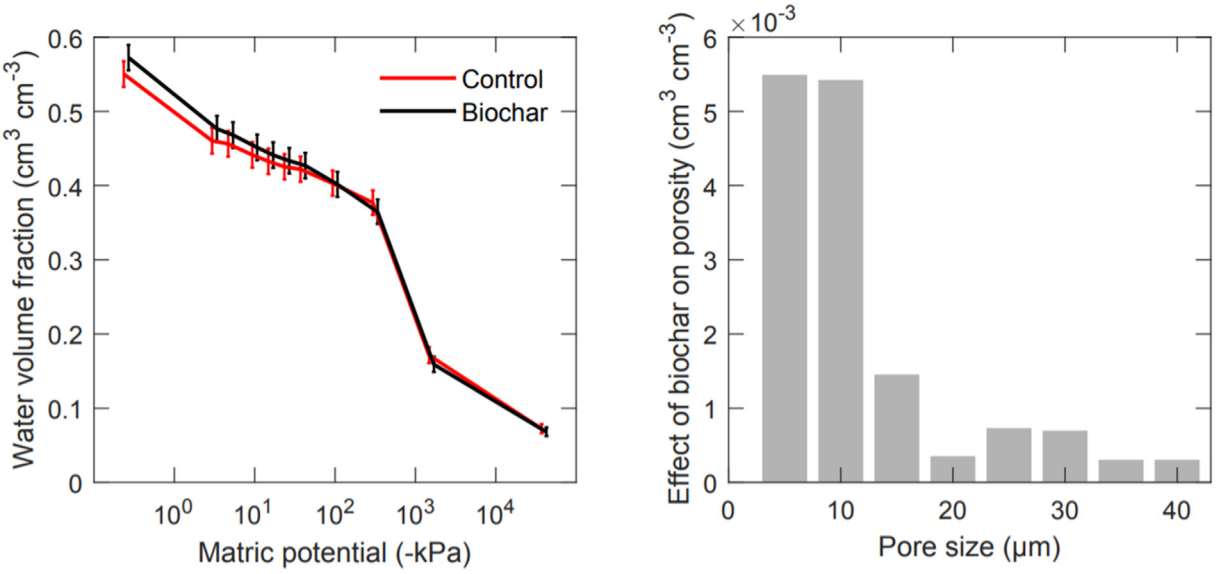

Fig. 2. Soil moisture characteristic curves of samples with and without (control) BC (estimated mean and 95% confidence intervals) and the effect of BC on soil porosity.

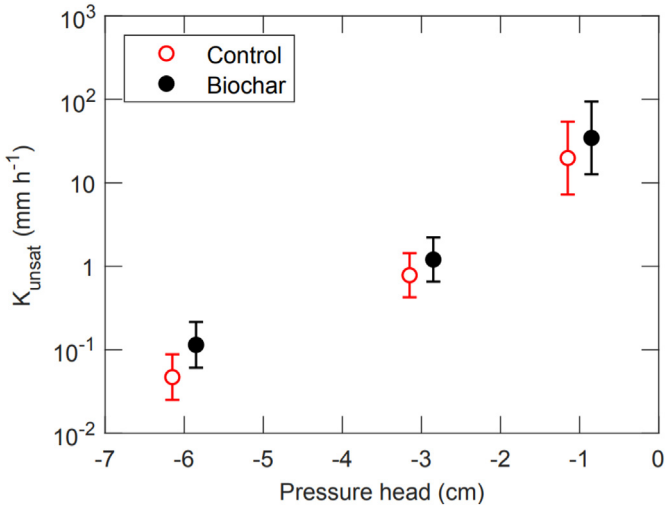

Fig. 3. Near-saturated hydraulic conductivity (K_{unsat}) in the control and BC-amended plots (mean and 95% confidence intervals) as measured in field in 2018.

while in samples S2 and S3, the corresponding diameter range was 20–25 µm.

3.6. Aggregate stabilities and rainfall simulation

BC application did not increase WSA%. In fact, the test indicated somewhat lower aggregate stability in BC-amended plots (WSA 79%, confidence interval 77–80%) compared to the control plots (WSA 82%, confidence interval 81-84%) ($p = 0.007$). It should be notet that for the BC treatment, the mass of soil was lower because of dilution by BC. Calculating WSA% based on the soil mass (BC subtracted from the mass weighted for the tests), there was no difference in the WSA% between the BC-amended and control soils ($p = 0.10$). Similarly, the detachment of colloidal particles during the wet-sieving procedure suggested that forest residue BC did not increase soil aggregate stability. Turbidity values measured for control and BC-amended plots were 30 and 36 NTU g^{-1} respectively ($p = 0.045$). Thus, a somewhat larger number of colloidal

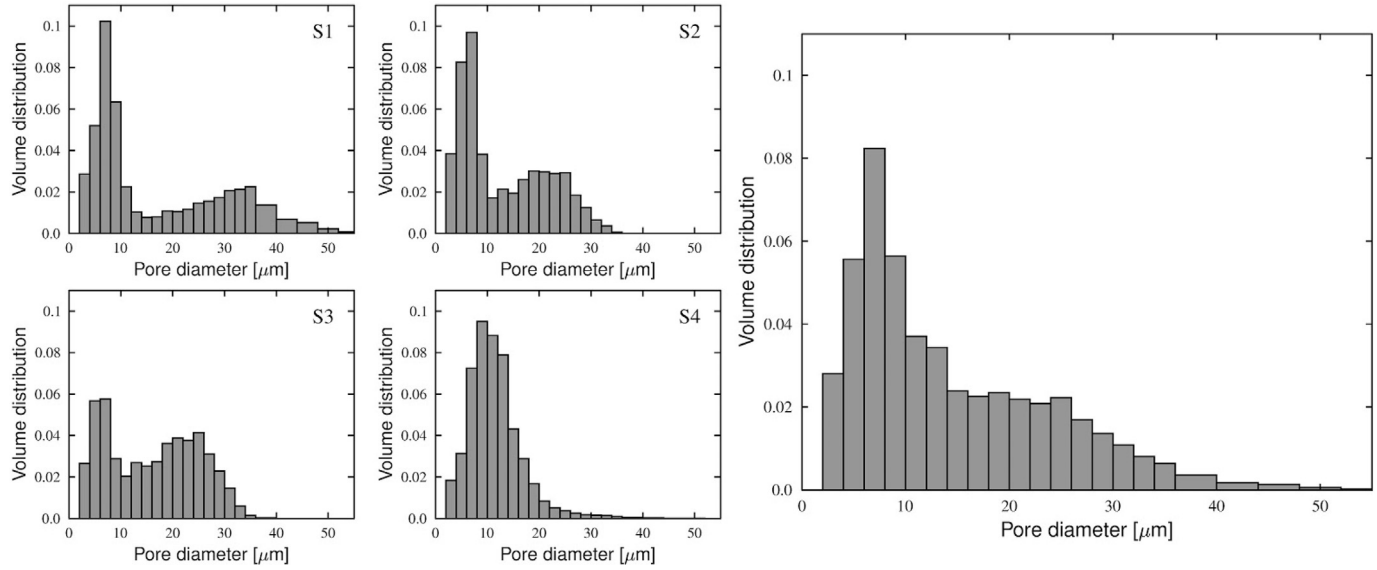

Fig. 4. Left: Pore size distributions of the four analyzed BC samples (S1-S4). Right: Pore size distribution combining the four individual BC samples.

Table 4
Means of pH, turbidity (NTU), and nutrient concentrations (mg l^{-1}) (dissolved organic carbon, DOC; ammonium, NH_4-N; nitrate, NO_3-N; total nitrogen, TN; dissolved phosphate, DRP; total phosphorus, TP) in drainage water collected in the rain simulation experiment from forest residue biochar (BC)-amended and control soils in 2017 and 2018. TP and turbidity were analyzed with gamma and lognormal distributions respectively. CI = confidence interval.

	2017				2018				*p* values of F-test		
	Control	CI	BC	CI	Control	CI	BC	CI	Treatment	Year	Interaction
pH	7.2	[7.1, 7.3]	7.3	[7.1, 7.4]	7.3	[7.2, 7.4]	7.4	[7.3, 7.5]	0.089	0.077	0.881
DOC	21	[15, 26]	23	[17, 29]	30	[28, 32]	28	[26, 30]	0.845	0.008	0.397
NH_4	0.15	[0.07, 0.24]	0.16	[0.06, 0.26]	0.30	[0.21, 0.38]	0.31	[0.23, 0.39]	0.820	0.009	0.941
NO_3	9.0	[4.6, 13.4]	6.3	[1.5, 11.1]	4.5	[3.3, 5.7]	3.4	[2.2, 4.7]	0.251	0.02	0.53
TN	11	[7.3, 15.2]	8.5	[4.2, 12.8]	7.4	[6.3, 8.4]	6.7	[5.6, 7.8]	0.253	0.036	0.375
DRP	0.06	[0.04, 0.09]	0.08	[0.05, 0.11]	0.16	[0.08, 0.23]	0.12	[0.04, 0.20]	0.725	0.076	0.363
TP	1.4	[1.2, 1.8]	1.8	[1.4, 2.3]	1.5	[1.2, 1.8]	1.8	[1.4, 2.2]	0.059	0.986	0.776
Turbidity	1009	[800, 1271]	1180	[852, 1467]	665	[527, 838]	827	[656, 1043]	0.167	0.019	0.644

size particles were detached from BC-treated soil than from the control soil.

The data obtained in rainfall simulations was in line with the aggregate stability tests. In rainfall simulations, the parameters associated with aggregate stability, turbidity, and TP concentration had *p*-values of 0.167 and 0.059 respectively (Table 4). Hence, BC did not improve the stability of surface soil toward raindrop impact, but TP and the turbidity of percolation water were slightly higher for the monoliths cored from BC-treated plots than those of the control plots in both years. The only positive indication that BC would be beneficial for water protection was that the NO_3-N concentration (and therefore also TN) of percolation water was lower than in water percolated through the control soil, but these effects also lacked statistical significance (Table 4).

3.7. Basal respiration and microbial community composition

Measured in the second year of the study, microbiological activity (basal respiration) was higher in the spring in the BC-treated plots than in the control plots, but no differences in respiration were measured later in the fall. There were no differences in fungal ITS, bacterial, or archaeal 16S rRNA gene copy amounts between treatments (Supplementary material 4).

The microbial biomass measures obtained from the PLFA analyses did not differ between the treatments (ANOVA) either: We measured 150, 60, and 4 nmol g^{-1} soil dw for $PLFA_{tot}$, $PLFA_{bact}$, and $PLFA_{fung}$ respectively (Table 5). The PCA analysis performed for the area% of each PLFA showed no treatment-related significant differences in the microbial community structure at the $p < 0.05$ level (ANOVA) (Supplementary material 5).

There were 12,652 and 21,462 assembled and quality filtered bacterial reads affiliating to 871 and 885 OTUs in samples from control and BC-treated plots respectively. More than half the bacterial reads for both control and BC amendment samples were clustered into Gammaproteobacteria (14%), Alphaproteobacteria (13%), Actinobacteria (9%), Gemmatimonadetes (8%), and Verrucomicrobiae (7%), while 11% remained unidentified at class level. At family level, the largest group of reads remained unidentified (33%), while the largest identified groups were Gemmatimonadaceae (8%), Chthoniobacteraceae (5%), Sphingomonadaceae (5%), Solibacteraceae (Subgroup 3) (3%), Xanthobacteraceae (3%), Intrasporangiaceae (3%), Burkholderiaceae (3%), Chitinophagaceae (2%), and Isosphaeraceae (2%) (Supplementary material 6). No trends toward shifts in bacterial community composition between control and BC-amended plots could be detected.

Table 5
Total microbial PLFAs (nmol g^{-1} soil) in control and in forest residue biochar- (BC) treated soils. CI = confidence interval.

	Control	CI	BC	CI	*p*
Total PLFAs	159	[123, 196]	158	[121, 195]	0.955
Fungi	4.1	[3.1, 5.0]	4.2	[3.2, 5.2]	0.800
Bacteria	66	[50, 81]	64	[49, 80]	0.905
B:F ratio	16	[14, 19]	15	[13, 18]	0.562

After assembly and quality filtering, there were 22,416 and 21,877 reads affiliated to 287 and 286 fungal OTUs in samples from control and BC-amended plots respectively. More than 60% of the fungal reads for both control and BC-amended samples were clustered into Ascomycota – 21% to Basidiomycota, and 0.1% to Glomeromycota. At family level, the largest group of reads were clustered into Thelebolaceae (20%), Piskurozymaceae (13%), Mortierellaceae (10%), and Pyrenomataceae (8%), while 8% remained unidentified (Supplementary material 6). Even at species level, there were no major shifts in fungal communities between control and BC plots (data not shown). Root symbiotic arbuscular mycorrhizal fungi were equally infrequent in both BC and control samples. Sequences from Claroideoglomeraceae, Paraglomeraceae, and Glomeraceae families comprised <0.1% of all reads. However, *Glomus* sp. Glomeraceae was three times more abundant in BC than in the control.

4. Discussion

4.1. Forest residue biochar and soil productivity

Forest residue BC did not affect the oat yields in the two years following the fall application. Similar results have been reported in other short-term biochar field experiments in Northern Europe (Tammeorg et al., 2014b Nelissen et al., 2015; O'Toole et al., 2018), as well as in mesocosm experiments (Borchard et al., 2014). However, when observed, it has been suggested increases in yields result from an increase in pH (Major et al., 2010; Vaccari et al., 2011), increased nutrient availability (Major et al., 2010), and relieved water deficit (Sohi et al., 2010; Jeffery et al., 2011). The major elements in the oat seeds were unaffected by the BC addition. The BC treatment slightly increased the Zn content and decreased the Ni content, but the differences between the treatments were significantly smaller than the variation between years. The increase in Mo content was significant in the first harvest after the BC treatment, supporting the findings of Rondon et al. (2007), which show a higher Mo uptake of non-N-fixing beans growing on a biochar-treated soil.

Acidic soils commonly benefit from lime application and an increase in pH. Though BC used in this experiment had pH of 8.4 it did not clearly increase the soil pH and no beneficial effects on yields could have been expected. The relatively high C and clay content of the experimental field indicates high buffering capacity against changes in pH which might explain the lack of effect of BC on pH. Of the measured plant available nutrients, BC only increased Ca and P in the surface soil. Major et al. (2010) found maize yields to be higher in biochar-amended plots after the first year and attributed the higher yields to the greater availability of Ca and Mg in soil where biochar was applied. However, it is unlikely that a higher Ca in BC-amended soils would have had the potential to

increase yields in the current study, because according to the Finnish fertility assessment, the Ca status of the soil was "satisfactory", and the Mg status of the soils was "good" or even "high". Furthermore, no differences were detected in Ca content in oat seeds between the BC-amended and control plots. Similarly, STP was "satisfactory" and at a level at which no yield increase due to P fertilization would be expected (Valkama et al., 2011).

One of the mechanisms behind the biochar-induced yield increases is the positive effect of biochar on soil water holding capacity (Jeffery et al., 2011). However, the reported effects vary, depending on the soil type, and study design or method. According to Tammeorg et al. (2014a), studies using undisturbed samples from field experiments show mixed results, whereas when repacked soil columns have been used, the results have often shown a biochar-induced increase in water holding capacity. This difference likely originates from more uniform distribution of biochar in experiments conducted in the laboratory whereas in the field a full range of interactions with soil, plants and soil biota takes place and thus, higher biochar application rates may be needed for some of its effects to become evident (Tammeorg et al., 2014a).

The pore structure of the forest residue BC revealed potential for water retention, and the porosity was in the same range as reported by Hyväluoma et al. (2018) for various biochars (0.34–0.68), Jeffery et al., 2015 for herbaceous biochar (0.48–0.57) and Berhanu et al. (2018) for wood-based biochar (0.50–0.58). The inherent heterogeneity of forest residue containing an unknown mix of of different tree species is reflected in BC pore structure as a variation.

When the pore size distributions of the four imaged samples were combined, the resulting distribution had a single clear peak at a pore diameter of 5–10 μm with a tail of up to 50 μm. This combined distribution suggests that BC derived from heterogeneous feedstock not only affects the water retention properties at a certain matric potential value (cf. e.g. Rasa et al., 2018) but at a wider range of potential. However, the water characteristic curve showed no clear difference between the BC-amended and control plots, but only a slight increase in the share of pores smaller than 10 μm and pores with a diameter around 25–30 μm occurred. These pore size regimes correspond to the pore size distribution of three of the four analyzed BC samples. This supports the findings suggesting that biochar affects soil moisture characteristics directly via its internal porosity (Rasa et al., 2018). In addition to the micrometer-scale porosity considered here, biochar also contains pyrogenic nanometer-scale porosity. This porosity contributes only minimally to the total porosity (Gray et al., 2014) and, in addition, pores smaller than 200 nm are not able to store plant available water. Therefore, the effect of nanometer-sale pores on water retention is minor.

Amending topsoil with biochar is known to reduce soil bulk density at the soil surface (Zhang et al., 2012; Mukherjee and Lal, 2013). The lower bulk densities in the 0–10 cm layer point toward increased porosity in BC-amended plots, but this was not supported by the water retention properties, because the water retention curve of BC-amended plots did not significantly differ from the control plots. Indeed, the total porosity of the BC was close to that of the unamended field soil and therefore the porosity of the mixture of soil and BC would not significantly differ from pure soil. The significantly lower bulk densities probably originate from mixing the lower density material in the clayey soil, with no significant changes in aggregate structure. However, it is reasonable to assert that changes in the soil's physical properties due to BC addition depend on soil type, while BC's capacity to store water in its internal structure is immutable (as long as BC quality remains the same).

4.2. Forest residue biochar and surface water quality

Low permeability of surface soil increases the risk of surface runoff and losses of nutrients to surface waters. BC addition has been reported to reduce the saturated hydraulic conductivity in sandy soil, whereas in clay soils, conductivity increases (Barnes et al., 2014). It is suggested that the increase in water infiltration of clayey soils originates in the lower bulk density resulting from increased porosity in BC-treated soils (Barnes et al., 2014). BC reduced the surface soil bulk density of the BC-treated plots in the current study, but near-saturated hydraulic conductivity did not significantly increase, suggesting that the BC addition's potential to reduce the risk of surface runoff was not great.

The aggregate stability of the clay soil in the field experiment was not improved over the 1.5-year study period, which is in line with previous studies that also failed to find positive effects of biochar amendments on aggregate stability (O'Toole et al., 2018; Heikkinen et al., 2019; Zhang et al., 2015). The relatively high charring degree of BC makes biochar a chemically inactive material, providing only a few sites for cation bridging and ligand exchange (Heikkinen et al., 2019), known to be important abiotic mechanisms for aggregate formation (Six et al., 2004). Furthermore, BC did not significantly affect soil bacteria or fungi, and thus, the widely reported microbe-induced increase in aggregate stability (Six et al., 2004; Cosentino et al., 2006) could not be expected. Instead, the detachment of colloid-size particles during wet sieving increased in samples from the BC-treated plots. The export of TP was shown to increase slightly after the BC addition, and as there was no change in the leaching of DRP, these results point toward the increased mobility of particle-bound P. The results suggest that BC does not have the potential to reduce erosion and the loss of particle bound P to surface waters.

Variable results on the effect of biochar on P solubility and on the risk of P loss to surface waters has been reported (Novak et al., 2009; Saarnio et al., 2018). BC has been suggested to act as sorptive surface for P (Novak et al., 2009) whereas Saarnio et al. (2018) have reported a biochar-induced increase in DRP concentration and loss in surface runoff. The increased P solubility in biochar-amended soils probably results from an increase in soil pH due to the biochar addition (Soinne et al., 2014; Saarnio et al., 2018) or from water-soluble P included in the biochar (Schnell et al., 2012). Although the pH increase was not significant in this field experiment, the solubility of P (P_{AAAc}) increased in the BC-treated plots. However, the increased solubility of P did not enhance the leaching of DRP in the rain simulation experiment. In a lysimeter experiment by Novak et al. (2009), the BC application increased P solubility (Mehlich1-P) in soil, but the P concentrations in leaching water decreased in the BC-treated plots. The effect of BC on DRP export is likely to differ, depending on the transportation route. Increased solubility of P in the surface soil originating from an increase in pH increases the risk of greater P loss through surface runoff. However, while water percolates through the soil profile toward artificial drains, the P solubilized from the surface soil is more likely to be sorbed into mineral or BC particles. However, the ability of biochar to participate in sorption reactions strongly depends on the raw material and pyrolysis process (Heikkinen et al., 2019).

In contrast with previous findings (Barnes et al., 2014; Bu et al., 2017; Saarnio et al., 2018; Borchard et al., 2019), the rain simulation experiments showed no changes in N leaching in two sequential springs after a single application of the BC in the fall. It has been suggested that the ability of biochar to reduce N leaching originates in the sorption of NH_4^+ and/or NO_3^- into BC particles (Wang et al., 2015) or increased biological activity leading to the immobilization of N (Bruun et al., 2012). Indeed, the respiration measurement showed higher microbiological activity in the BC-amended soils in the spring, which may suggest increased nitrogen immobilization. However, the higher respiration is also related to the increased mineralization of natural organic C and N, which could lead to increase in dissolved N (NH_4^+, NO_3^-) concentrations in soil water. Possible effects of BC on N leaching might have been masked by large variation in soil monoliths and mobilization of soluble N below the uppermost 10 cm of soil where the BC was mixed. Thus, BC mixed in the soil surface did not significantly reduce the N concentrations in percolating water, but this experimental setup does not allow us to conclude on the possible effects of BC on the N concentrations in

the surface runoff water. Given that BC did not affect infiltration, increase aggregate stability, or reduce the colloid detachment, and increased the solubility of STP in the surface soil, the application of BC cannot be recommended as a measure to quickly reduce P losses.

4.3. Carbon sequestration potential

In BC-treated soil, C content increased significantly only in the soil's topmost layer, which is well in line with the shallow cultivation and short experimental period. Although the determination of soil C storage and its changes due to soil amendments hold various uncertainties (Poulton et al., 2018), the present data suggest a 19 Mg ha^{-1} increase in soil C in the topmost 45 cm. This would be 79% of the 24 Mg C ha^{-1} introduced in the BC amendment. The fate of the remaining 5 Mg ha^{-1} of the added C is open, but C can be lost via decomposition, leaching, or migration due to cultivation practices. Possible uncertainties in sampling and analysis may also contribute to the observed deficit. Liu et al. (2016) reported accelerated leaching of C in a field plot scale study even after a year of biochar application. However, in our rain simulation study, the DOC concentration in leaching water did not differ between the BC and control plots. This suggests that BC does not contribute to maintaining higher DOC concentrations in drainage water, and that if C is lost through leaching, export should readily occur after the application to the field.

Most of the biochar is generally considered to be largely unavailable for microbial degradation (Lehmann et al., 2011). However, increases in respiration and microbial biomass in biochar-amended soils have been reported (Sheng and Zhu, 2018), but in many cases, the increase in CO_2 emissions has been temporary (Novak et al., 2010; Smith et al., 2010). The microbial decomposition of easily degradable fractions of biochar is fastest after the biochar addition, which may explain at least part of the C lost within the first years (Bird et al., 2015). In acidic soils, the increase in CO_2 emissions has been suggested to originate from a biochar-induced increase in soil pH, leading to increased bacterial diversity, while in alkaline soils, no change in CO_2 emissions has been detected (Sheng and Zhu, 2018). The higher respiration in biochar-treated soils may originate from labile organic compounds added to soil with biochar, and the biochar addition may even result in negative priming of natural SOM and therefore contribute to restoring native C in more stable form (Zheng et al., 2018). According to Zheng et al. (2018), the reduction in the mineralization of natural SOM in biochar-treated soils resulted from improved aggregate stability and changes in the microbial C use efficiency and community composition. In the present study, BC had no effect on soil pH, and the increase in basal respiration was detected only in the spring samples taken before the second growth season after BC addition. Furthermore, the aggregate stability was not affected by the relatively well carbonized BC. According to the recent review of Palansooriya et al. (2019), the effects of biochar on microbial biomass and community composition may also originate from increased porosity. However, the porosity of the BC was fairly similar to the clay soil in the field, and the BC addition did not result in a significant increase in the pore volume. Given that the BC had minor effects on soil physical and chemical properties, and it is stable against microbiological decomposition, the insignificant response in microbiological factors is not surprising. Thus, we agree with the recent critical review that in studying the effects of biochar on microbiomes, various types of biochar, different biochar application rates, and different plant species for assessing the magnitude of biochar effects on soil microorganisms over time and under different conditions must be considered (Palansooriya et al., 2019).

The H:C and O:C molar ratios (0.46 and 0.09 respectively) suggest that the BC used in the experiment was relatively well carbonized and stable against degradation. According to Spokas (2010), the estimated half-life of biochars with an O:C ratio lower than 0.2 may exceed 1000 years. It is therefore likely that the BC could be stored in the soil for several hundred years. However, it should be underlined that the C sequestration potential of the BC used in the present experiment relies solely on the recalcitrant nature of the pyrolyzed biomass. Woolf et al. (2010) addressed the importance of the field's improved growing conditions and the consequent higher C return to the soil. The results of our experiment did not indicate any changes in yield, or any soil parameters that would clearly allow us to forecast a higher biomass production and consequent additional increase in C sequestration in the coming years.

5. Conclusions

Short-term environmental and economic benefits are fundamental factors justifying wide-scale biochar use in agriculture. The amendment of boreal clay soil with a high dose of BC characterized by a moderately alkaline pH, low surface functionalities, and recalcitrant nature induced no immediate positive impacts that would unambiguously motivate farmers to invest in BC. Minor positive signs detected in soil properties were concentrated in the soil's topmost layer, while yield did not increase. BC amendment showed no potential to reduce nutrient leaching from clay soil. Thus, the results do not support financial compensation by society for BC amendment (e.g. through the Common Agricultural Policy in EU countries). A positive consequence of BC use is increased C sequestration, which will probably lead to long-term C storage. Yet no negative effects were detected in this short-term field trial, suggesting that BC use poses no risk to agricultural soil or the environment. However, the present study includes only one biochar and soil type, and considering the variability in biochars, caution must be exercised in generalizing the results.

Supplementary data to this article can be found online at https://doi.org/10.1016/j.scitotenv.2020.138955.

CRediT authorship contribution statement

Helena Soinne: Investigation, Formal analysis, Writing - original draft, Writing - review & editing. **Riikka Keskinen:** Conceptualization, Investigation, Writing - original draft, Writing - review & editing. **Jaakko Heikkinen:** Investigation, Formal analysis, Visualization, Writing - review & editing. **Jari Hyväluoma:** Conceptualization, Investigation, Formal analysis, Writing - review & editing. **Risto Uusitalo:** Investigation, Supervision, Writing - review & editing. **Krista Peltoniemi:** Investigation, Writing - review & editing. **Sannakajsa Velmala:** Investigation, Writing - review & editing. **Taina Pennanen:** Investigation, Writing - review & editing. **Hannu Fritze:** Investigation, Resources, Supervision, Writing - review & editing. **Janne Kaseva:** Formal analysis, Writing - review & editing. **Markus Hannula:** Investigation, Resources. **Kimmo Rasa:** Project administration, Conceptualization, Funding acquisition, Resources, Writing - review & editing.

Declaration of competing interest

The authors declare that they have no known competing financial interests or personal relationships that could have appeared to influence the work reported in this paper.

Acknowledgement

We thank Tuija Hytönen and Juha-Matti Pitkänen for their excellent technical assistance in preparing soil samples for DNA extractions, amplicon sequencing, and qPCR, Maija Ruokolainen for her basal respiration measurements, and Pia Grandell for her PLFA work. Anssi Källi from the VTT Technical Research Centre of Finland is acknowledged for his CHN analyses. This project received funding from the European Union's Horizon 2020 research and innovation program under grant agreement No. 637020—MOBILEFLIP, as well as from the Ministry of Education and Culture, Finland, project Bioproduct and Clean Bioeconomy – RDI FlagShip in Xamk.

References

Abel, S., Peters, A., Trinks, S., Schonsky, H., Facklam, M., Wessolek, G., 2013. Impact of biochar and hydrochar addition on water retention and water repellency of sandy soil. Geoderma 202–203, 183–191.

Ankeny, M.D., Ahmed, M., Kaspar, T.C., Horton, R., 1991. Simple field method for determining unsaturated hydraulic conductivity. Soil Sci. Soc. Am. J. 55, 467–470.

Anslan, S., Bahram, M., Hiiesalu, I., Tedersoo, L., 2017. PipeCraft: flexible open-source toolkit for bioinformatics analysis of custom high-throughput amplicon sequencing data. Mol. Ecol. Resour. 17, e234–e240. https://doi.org/10.1111/1755-0998.12692.

Atkinson, C.J., Fitzgerald, J.D., Hipps, N.A., 2010. Potential mechanisms for achieving agricultural benefits from biochar application to temperate soils: a review. Plant Soil 337, 1–18.

Barnes, R.T., Gallagher, M.E., Masiello, C.A., Liu, Z., Dugan, B., 2014. Biochar-induced changes in soil hydraulic conductivity and dissolved nutrient fluxes constrained by laboratory experiments. PLoS One 9, e108340. https://doi.org/10.1371/journal.pone.0108340.

Bengtsson-Palme, J., Ryberg, M., Hartmann, M., Branco, S., Wang, Z., Godhe, A., De Wit, P., Sánchez-García, M., Ebersberger, I., de Sousa, F., Amend, A., 2013. Improved software detection and extraction of ITS1 and ITS 2 from ribosomal ITS sequences of fungi and other eukaryotes for analysis of environmental sequencing data. Methods Ecol. Evol. 4, 914–919. https://doi.org/10.1111/2041-210X.12073.

Berhanu, S., Hervy, M., Weiss-Hortala, E., Proudhon, H., Berger, M.H., Chesnaud, A., Faessel, M., King, A., Minh, D.P., Villot, A., Gerente, C., 2018. Advanced characterization unravels the structure and reactivity of wood-based chars. Journal of Analytical and Applied Pyrolysis 130, 79–89.

Bird, M.I., Wynn, J.G., Saiz, G., Wurster, C.M., McBeath, A., 2015. The pyrogenic carbon cycle. Annu. Rev. Earth Planet. Sci. 43 (1), 273–298.

Boehm, H.-P., Diehl, E., Heck, W., Sappok, R., 1964. Surface oxides of carbon. Angew. Chem. Int. Ed. 3, 669–677.

Borchard, N., Wolf, A., Laabs, V., Aeckersberg, R., Scherer, H.W., Moeller, A., Amelung, W., 2012. Physical activation of biochar and its meaning for soil fertility and nutrient leaching–a greenhouse experiment. Soil Use Manag. 28 (2), 177–184.

Borchard, N., Siemens, J., Ladd, B., Möller, A., Amelung, W., 2014. Application of biochars to sandy and silty soil failed to increase maize yield under common agricultural practice. Soil Tillage Res. 144, 184–194.

Borchard, N., Schirrmann, M., Cayuela, M.L., Kammann, C., Wrage-Mönnig, N., Estavillo, J.M., Fuertes-Mendizábal, T., Sigua, G., Spokas, K., Ippolito, J.A., Novak, J., 2019. Biochar, soil and land-use interactions that reduce nitrate leaching and N2O emissions: a meta-analysis. Sci. Total Environ. 651, 2354–2364.

Brassard, P., Godbout, S., Raghavan, V., 2016. Soil biochar amendment as a climate change mitigation tool: key parameters and mechanisms involved. J. Environ. Manag. 181, 484–497.

Bruun, E.W., Ambus, P., Egsgaard, H., Hauggaard-Nielsen, H., 2012. Effects of slow and fast pyrolysis biochar on soil C and N turnover dynamics. Soil Biol. Biochem. 46, 73–79.

Bu, X., Xue, J., Zhao, C., Wu, Y., Han, F., 2017. Nutrient leaching and retention in riparian soils as influenced by rice husk biochar addition. Soil Sci. 182 (7), 241–247.

Caporaso, J.G., Lauber, C.L., Walters, W.A., Berg-Lyons, D., Lozupone, C.A., Turnbaugh, P.J., Fierer, N., Knight, R., 2011. Global patterns of 16S rRNA diversity at a depth of millions of sequences per sample. Proc. Natl. Acad. Sci. 108 (Supplement 1), 4516–4522. https://doi.org/10.1073/pnas.1000080107.

Caporaso, J.G., Lauber, C.L., Walters, W.A., Berg-Lyons, D., Huntley, J., Fierer, N., Owens, S.M., Betley, J., Fraser, L., Bauer, M., Gormley, N., 2012. Ultra-high-throughput microbial community analysis on the Illumina HiSeq and MiSeq platforms. ISME J. 6 (8), 1621–1624. https://doi.org/10.1038/ismej.2012.8.

Chan, K.Y., Van Zwieten, L., Meszaros, I., Downie, A., Joseph, S., 2008. Using poultry litter biochars as soil amendments. Aust. J. Soil Res. 46, 437–444.

Chintala, R., Schumacher, T.E., Kumar, S., Malo, D.D., Rice, J.A., Bleakley, B., Chilom, G., Clay, D.E., Julson, J.L., Papiernik, S.K., Gu, Z.R., 2014. Molecular characterization of biochars and their influence on microbiological properties of soil. J. Hazard. Mater. 279, 244–256.

Cosentino, D., Chenu, C., Le Bissonnais, Y., 2006. Aggregate stability and microbial community dynamics under drying–wetting cycles in a silt loam soil. Soil Biol. Biochem. 38 (8), 2053–2062.

Federle, T.W., 1986. Microbial distribution in soil – new techniques. In: Megusar, F., Gantar, M. (Eds.), Perspectives in Microbial Ecology. Slovene Society for Microbiology, Ljubljana, pp. 493–498.

Frostegård, Å., Bååth, E., 1996. The use of phospholipid fatty acid analysis to estimate bacterial and fungal biomass in soil. Biol. Fertil. Soils 22, 59–65.

Frostegård, Å., Bååth, E., Tunlid, A., 1993. Shifts in the structure of soil microbial communities in limed forests as revealed by phospholipid fatty acid analysis. Soil Biol. Biochem. 25, 723–730.

Fu, L., Niu, B., Zhu, Z., Wu, S., Li, W., 2012. CD-HIT: accelerated for clustering the next-generation sequencing data. Bioinformatics 28, 3150–3152.

Gbur, E.E., Stroup, W.W., McCarter, K.S., Durham, S., Young, L.J., Christman, M., West, M., Kramer, M., 2012. Analysis of Generalized Linear Mixed Models in the Agricultural and Natural Resources Sciences. John Wiley & Sons.

Gomez, J.D., Denef, K., Stewart, C.E., Zheng, J., Cotrufo, M.F., 2014. Biochar addition rate influences soil microbial abundance and activity in temperate soils. Eur. J. Soil Sci. 65, 28–39.

Gonzalez, R.C., Woods, R.E., 2001. Digital Image Processing. 2nd ed. Addison-Wesley, Boston, MA, USA, p. 2001.

Gray, M., Johnson, M.G., Dragila, M.I., Kleber, M., 2014. Water uptake in biochars: the roles of porosity and hydrophobicity. Biomass Bioenergy 61, 196–205.

Heikkinen, J., Keskinen, R., Soinne, H., Hyväluoma, J., Nikama, J., Wikberg, H., Källi, A., Siipola, V., Melkior, T., Dupont, C., Campargue, M., 2019. Possibilities to improve soil aggregate stability using biochars derived from various biomasses through slow pyrolysis, hydrothermal carbonization, or torrefaction. Geoderma 344, 40–49.

Hilpert, M., Glantz, R., Miller, C.T., 2003. Calibration of a pore-network model by a pore-morphological analysis. Transp. Porous Media 51, 267–285.

Horgan, G.W., 1998. Mathematical morphology for analysing soil structure from images. Eur. J. Soil Sci. 49, 161–173.

Hyväluoma, J., Kulju, S., Hannula, M., Wikberg, H., Källi, A., Rasa, K., 2018. Quantitative characterization of pore structure of several biochars with 3D imaging. Environ. Sci. Pollut. Res. 25, 25648–25658.

Ihrmark, K., Bödeker, I., Cruz-Martinez, K., Friberg, H., Kubartova, A., Schenck, J., Strid, Y., Stenlid, J., Brandström-Durling, M., Clemmensen, K.E., Lindahl, B.D., 2012. New primers to amplify the fungal ITS2 region–evaluation by 454-sequencing of artificial and natural communities. FEMS Microbiol. Ecol. 82 (3), 666–677. https://doi.org/10.1111/j.1574-6941.2012.01437.x.

Jeffery, S., Verheijen, F.G., van der Velde, M., Bastos, A.C., 2011. A quantitative review of the effects of biochar application to soils on crop productivity using meta-analysis. Agric. Ecosyst. Environ. 144 (1), 175–187.

Jeffery, S, Meinders, M.B, Stoof, C.R, Bezemer, T.M, van de Voorde, T.F, Mommer, L, van Groenigen, J.W, 2015. Biochar application does not improve the soil hydrological function of a sandy soil. Geoderma 251, 47–54.

Jeffery, S., Abalos, D., Prodana, M., Bastos, A.C., Van Groenigen, J.W., Hungate, B.A., Verheijen, F., 2017. Biochar boosts tropical but not temperate crop yields. Environ. Res. Lett. 12 (5), 053001.

Kavitha, B., Reddy, P.V.L., Kim, B., Lee, S.S., Pandey, S.K., Kim, K.H., 2018. Benefits and limitations of biochar amendment in agricultural soils: a review. J. Environ. Manag. 227, 146–154.

Kenward, M.G., Roger, J.H., 2009. An improved approximation to the precision of fixed effects from restricted maximum likelihood. Comput. Stat. Data Anal. 53, 2583–2595.

Kim, Y.S., Yang, S.J., Lim, H.J., Kim, T., Park, C.R., 2012. A simple method for determining the neutralization point in Boehm titration regardless of the CO2 effect. Carbon 50, 3315–3323.

Kõljalg, U., Nilsson, R.H., Abarenkov, K., Tedersoo, L., Taylor, A.F., Bahram, M., Bates, S.T., Bruns, T.D., Bengtsson-Palme, J., Callaghan, T.M., Douglas, B., 2013. Towards a unified paradigm for sequence-based identification of fungi. Mol. Ecol. 22 (21), 5271–5277. https://doi.org/10.1111/mec.12481.

Laird, D.A., Fleming, P., Davis, D.D., Horton, R., Wang, B., Karlen, D.L., 2010. Impact of biochar amendments on the quality of a typical Midwestern agricultural soil. Geoderma 158, 443–449.

Le Bissonnais, Y., 1996. Aggregate stability and assessment of soil crustability and erodibility: I. Theory and methodology. Eur. J. Soil Sci. 47, 425–437.

Lee, Y., Park, J., Ryu, C., Gang, K.S., Yang, W., Park, Y.-K., Jung, J., Hyun, S., 2013. Comparison of biochar properties from biomass residues produced by slow pyrolysis at 500 °C. Bioresour. Technol. 148, 196–201.

Lehmann, J., 2007. A handful of carbon. Nature 447, 143–144.

Lehmann, J., Czimczik, C., Laird, D., Sohi, S., 2009. Stability of Biochar in Soil. Biochar for Environmental Management: Science and Technology. pp. 183–206.

Lehmann, J., Rillig, M.C., Thies, J., Masiello, C.A., Hockaday, W.C., Crowley, D., 2011. Biochar effects on soil biota - a review. Soil Biol. Biochem. 43, 1812–1836.

Lilja, H., Uusitalo, R., Yli-Halla, M., Nevalainen, R., Väänänen, T., Tamminen, P., Tuhtar, J., 2017. Suomen maannostietokanta: Käyttöopas versio 1.1. Luonnonvara- ja biotalouden tutkimus 6/2017 in Finnish.

Liu, X., Zhang, A., Ji, C., Joseph, S., Bian, R., Li, L., Pan, G., Paz-Ferreiro, J., 2013. Biochar's effect on crop productivity and the dependence on experimental conditions – a meta-analysis of literature data. Plant Soil 373, 583–594.

Liu, C., Wang, H., Tang, X., Guan, Z., Reid, B.J., Rajapaksha, A.U., Ok, Y.S., Sun, H., 2016. Biochar increased water holding capacity but accelerated organic carbon leaching from a sloping farmland soil in China. Environ. Sci. Pollut. Res. 23 (2), 995–1006.

Lu, S.-G., Sun, F.-F., Zong, Y.-T., 2014. Effect of rice husk biochar and coal fly ash on some physical properties of expansive clayey soil (Vertisol). Catena 114, 37–44.

Major, J., Rondon, M., Molina, D., Riha, S.J., Lehmann, J., 2010. Maize yield and nutrition during 4 years after biochar application to a Colombian savanna oxisol. Plant Soil 333, 117–128.

Matovic, D., 2011. Biochar as a viable carbon sequestration option: global and Canadian perspective. Energy 36, 2011–2016.

Mehlich, A, 1984. Mehlich 3 soil test extractant: A modification of Mehlich 2 xtractant. Communications in soil science and plant analysis 15, 1409–1416.

Mukherjee, A., Lal, R., 2013. Biochar impacts on soil physical properties and greenhouse gas emissions. Agronomy 3 (2), 313–339.

Nelissen, G. Ruysschaert, Manka'Abusi, D., D'Hose, T., De Beuf, K., Al-Barri, B., Cornelis, W., Boeckx, P., 2015. Impact of a woody biochar on properties of a sandy loam soil and spring barley during a two-year field experiment. Eur. J. Agron. 62, 65–78.

Nilsson, R.H., Larsson, K.-H., Taylor, A.F.S., Bengtsson-Palme, J., Jeppesen, T.S., Schigel, D., Kennedy, P., Picard, K., Glöckner, F.O., Tedersoo, L., Saar, I., Kõljalg, U., Abarenkov, K., 2018. The UNITE database for molecular identification of fungi: handling dark taxa and parallel taxonomic classifications. Nucleic Acids Res. https://doi.org/10.1093/nar/gky1022.

Novak, J.M., Busscher, W.J., Laird, D.L., Ahmedna, M., Watts, D.W., Niandou, M.A., 2009. Impact of biochar amendment on fertility of a southeastern coastal plain soil. Soil Sci. 174 (2), 105–112.

Novak, J.M., Busscher, W.J., Watts, D.W., Laird, D.A., Ahmedna, M.A., Niandou, M.A., 2010. Short-term CO2 mineralization after additions of biochar and switchgrass to a Typic Kandiudult. Geoderma 154 (3–4), 281–288.

O'Toole, A., Moni, C., Weldon, S., Schols, A., Carnol, M., Bosman, B., Rasse, D.P., 2018. Miscanthus biochar had limited effects on soil physical properties, microbial biomass, and grain yield in a four-year field experiment in Norway. Agriculture 8, 171.

Palansooriya, K.N., Wong, J.T.F., Hashimoto, Y., Huang, L., Rinklebe, J., Chang, S.X., Bolan, N., Wang, H., Ok, Y.S., 2019. Response of microbial communities to biochar-amended soils: a critical review. Biochar 1, 3–22.
Peltoniemi, K., Laiho, R., Juottonen, H., Kiikkilä, O., Mäkiranta, P., Minkkinen, K., Pennanen, T., Penttilä, T., Sarjala, T., Tuittila, E.-S., Tuomivirta, T., Fritze, H., 2015. Microbial ecology in a future climate: effects of temperature and moisture on microbial communities of two boreal fens. FEMS Microbiol. Ecol. 91. https://doi.org/10.1093/femsec/fiv062.
Pennanen, T., Liski, J., Bååth, E., Kitunen, V., Uotila, J., Westman, C.J., Fritze, H., 1999. Structure of microbial communities in coniferous forest soils in relation to site fertility and stand development stage. Microb. Ecol. 38, 168–179.
Persson, L., Bergström, L., 1991. Drilling method for collection of undisturbed soil monoliths. Soil Sci. Soc. Am. J. 55, 285–287.
Pietikäinen, J., Fritze, H., 1995. Clear-cutting and prescribed burning in coniferous forest: comparison of effects on soil fungal and total microbial biomass, respiration activity and nitrification. Soil Biol. Biochem. 27, 101–109.
Poulton, P., Johnston, J., Macdonald, A., White, R., Powlson, D., 2018. Major limitations to achieving "4 per 1000" increases in soil organic carbon stock in temperate regions: evidence from long-term experiments at Rothamsted Research, United Kingdom. Glob. Chang. Biol. 24, 2563–2584.
Quast, C., Pruesse, E., Yilmaz, P., Gerken, J., Schweer, T., Yarza, P., Peplies, J., Glöckner, F.O., 2012. The SILVA ribosomal RNA gene database project: improved data processing and web-based tools. Nucleic Acids Res. 41, D590–D596. https://doi.org/10.1093/nar/gks1219.
Rasa, K., Heikkinen, J., Hannula, M., Arstila, K., Kulju, S., Hyväluoma, J., 2018. How and why does willow biochar increase a clay soil water retention capacity? Biomass Bioenergy 119, 346–353.
Repo, A., Tuomi, M., Liski, J., 2011. Indirect carbon dioxide emissions from producing bioenergy from forest harvest residue. Glob. Chang. Biol. Bioenergy 3, 107–115. https://doi.org/10.1111/j.1757-1707.2010.01065.x.
Rognes, T., Flouri, T., Nichols, B., Quince, C., Mahé, F., 2016. VSEARCH: a versatile open source tool for metagenomics. PeerJ 4, e2584. https://doi.org/10.7717/peerj.2584.
Rondon, M.A., Lehmann, J., Ramirez, J., Hurtado, M., 2007. Biological nitrogen fixation by common beans (Phaseolus vulgaris L.) increases with biochar additions. Biol. Fertil. Soils 43, 699–708.
Ronsse, F., van Hecke, S., Dickinson, D., Prins, W., 2013. Production and characterization of slow pyrolysis biochar: influence of feedstock type and pyrolysis conditions. GCB Bioenergy 5, 104–115.
Routa, J., Asikainen, A., Björheden, R., Laitila, J., Röser, D., 2013. Forest energy procurement: state of the art in Finland and Sweden. WIREs Energy Environ. 2, 602–613. https://doi.org/10.1002/wene.24.
Saarnio, S., Räty, M., Hyrkäs, M., Virkajärvi, P., 2018. Biochar addition changed the nutrient content and runoff water quality from the top layer of a grass field during simulated snowmelt. Agric. Ecosyst. Environ. 265, 156–165.
Sauvola, J., Pietikäinen, M., 2000. Adaptive document image binarization. Pattern Recogn. 33, 225–236.
Schloss, P.D., Westcott, S.L., Ryabin, T., Hall, J.R., Hartmann, M., Hollister, E.B., Lesniewski, R.A., Oakley, B.B., Parks, D.H., Robinson, C.J., Sahl, J.W., 2009. Introducing mothur: open-source, platform-independent, community-supported software for describing and comparing microbial communities. Appl. Environ. Microbiol. 75, 7537–7541. https://doi.org/10.1128/AEM.01541-09.
Schnell, R.W., Vietor, D.M., Provin, T.L., Munster, C.L., Capareda, S., 2012. Capacity of biochar application to maintain energy crop productivity: soil chemistry, sorghum growth, and runoff water quality effects. J. Environ. Qual. 41, 1044–1051.
Sheng, Y., Zhu, L., 2018. Biochar alters microbial community and carbon sequestration potential across different soil pH. Sci. Total Environ. 622, 1391–1399.
Six, J., Bossuyt, H., Degryze, S., Denef, K., 2004. A history of research on the link between (micro) aggregates, soil biota, and soil organic matter dynamics. Soil Tillage Res. 79, 7–31.
Smith, P., 2016. Soil carbon sequestration and biochar as negative emission technologies. Glob. Chang. Biol. 22, 1315–1324.
Smith, J.L., Collins, H.P., Bailey, V.L., 2010. The effect of young biochar on soil respiration. Soil Biol. Biochem. 42, 2345–2347.
Sohi, S.P., Krull, E., Lopez-Capel, E., Bol, R., 2010. A review of biochar and its use and function in soil. Adv. Agron. 105, 47–82.
Soinne, H., Hovi, J., Tammeorg, P., Turtola, E., 2014. Effect of biochar on phosphorus sorption and clay soil aggregate stability. Geoderma 219, 162–167.
Sollins, P., Robertson, G.P., Uehara, G., 1988. Nutrient mobility in variable- and permanent-charge soils. Biogeochemistry 6, 181–199.
Spokas, K.A., 2010. Review of the stability of biochar in soils: predictability of O:C molar ratios. Carbon Manag. 1, 289–303.
Spokas, K.A., Cantrell, K.B., Novak, J.M., Archer, D.W., Ippolito, J.A., Collins, H.P., Boateng, A.A., Lima, I.M., Lamb, M.C., McAloon, A.J., Lentz, R.D., Nichols, K.A., 2012. Biochar: a synthesis of its agronomic impact beyond carbon sequestration. J. Environ. Qual. 41, 973–989.
Sun, Y., Gao, B., Yao, Y., Fang, J., Zhang, M., Zhou, Y., Chen, H., Yang, L., 2014. Effects of feedstock type, production method, and pyrolysis temperature on biochar and hydrochar properties. Chem. Eng. J. 240, 574–578.
Tammeorg, P., Simojoki, A., Mäkelä, P., Stoddard, F.L., Alakukku, L., Helenius, J., 2014a. Biochar application to a fertile sandy clay loam in boreal conditions: effects on soil properties and yield formation of wheat, turnip rape and faba bean. Plant Soil 374, 89–107.
Tammeorg, P., Simojoki, A., Mäkelä, P., Stoddard, F.L., Alakukku, L., Helenius, J., 2014b. Short-term effects of biochar on soil properties and wheat yield formation with meat bone meal and inorganic fertiliser on a boreal loamy sand. Agric. Ecosyst. Environ. 191, 108–116.
Uusitalo, R., Aura, E., 2005. A rainfall simulation study on the relationships between soil test P versus dissolved and potentially bioavailable particulate phosphorus forms in runoff. Agric. Food Sci. 14, 335–345.
Uusitalo, R., Ylivainio, K., Hyväluoma, J., Rasa, K., Kaseva, J., Nylund, P., Pietola, L., Turtola, E., 2012. The effects of gypsum on the transfer of phosphorus and other nutrients through clay soil monoliths. Agric. Food Sci. 21, 260–278.
Vaccari, F.P., Baronti, S., Lugato, E., Genesio, L., Castaldi, S., Fornasier, F., Miglietta, F., 2011. Biochar as a strategy to sequester carbon and increase yield in durum wheat. Eur. J. Agron. 34, 231–238. https://doi.org/10.1016/j.eja.2011.01.006.
Valkama, E., Uusitalo, R., Turtola, E., 2011. Yield response models to phosphorus application: a research synthesis of Finnish field trials to optimize fertilizer P use of cereals. Nutr. Cycl. Agroecosyst. 91, 1–15.
Van Zwieten, L., Kimber, S., Morris, S., Chan, K.Y., Downie, A., Rust, J., Joseph, S., Cowie, A., 2010. Effects of biochar from slow pyrolysis of papermill waste on agronomic performance and soil fertility. Plant Soil 327, 235–246.
Verheijen, F.G.A., Jeffery, S., Bastos, A.C., van der Velde, M., Diafas, I., 2009. Biochar Application to Soils - A Critical Scientific Review of Effects on Soil Properties, Processes and Functions. EUR 24099 EN, Office for the Official Publications of the European Communities, Luxembourg (149 pp.).
Vuorinen, J., Mäkitie, O., 1955. The Method of Soil Testing in Use in Finland. 63. Agrogeological Publications, pp. 1–44.
Wang, Z., Guo, H., Shen, F., Yang, G., Zhang, Y., Zeng, Y., Wang, L., Xiao, H., Deng, S., 2015. Biochar produced from oak sawdust by Lanthanum (La)-involved pyrolysis for adsorption of ammonium (NH4+), nitrate (NO3−), and phosphate (PO43-). Chemosphere 119, 646–653.
Wang, J., Xiong, Z., Kuzyakov, Y., 2016. Biochar stability in soil: meta-analysis of decomposition and priming effects. GCB Bioenergy 8, 512–523.
Westfall, P.H., 1997. Multiple testing of general contrasts using logical constraints and correlations. J. Am. Stat. Assoc. 92, 299–306.
White, T.J., Bruns, T., Lee, S., Taylor, J.W., 1990. Amplification and direct sequencing of fungal ribosomal RNA genes for phylogenetics. In: Innis, M.A., Gelfand, D.H., Sninsky, J.J., White, T.J. (Eds.), PCR Protocols: A Guide to Methods and Applications. 1990. Academic Press Inc., New York, pp. 315–322.
Windeatt, J.H., Ross, A.B., Williams, P.T., Forster, P.M., Nahil, M.A., Singh, S., 2014. Characteristics of biochars from crop residues: potential for carbon sequestration and soil amendment. J. Environ. Manag. 146, 189–197.
Wooding, R.A., 1968. Steady infiltration from a shallow circular pond. Water Resour. Res. 4, 1259–1273.
Woolf, D., Amonette, J., Street-Perrott, F., Lehmann, J., Joseph, S., 2010. Sustainable biochar to mitigate global climate change. Nat. Commun. 1, 56.
Yilmaz, P., Parfrey, L.W., Yarza, P., Gerken, J., Pruesse, E., Quast, C., Schweer, T., Peplies, J., Ludwig, W., Glöckner, F.O., 2014. The SILVA and "all-species living tree project (LTP)" taxonomic frameworks. Nucleic Acids Res. 42, D643–D648. https://doi.org/10.1093/nar/gkt1209.
Yu, H., Zou, W., Chen, J., Chen, H., Yu, Z., Huang, J., Tang, H., Wei, X., Gao, B., 2019. Biochar amendment improves crop production in problem soils: a review. J. Environ. Manag. 232, 8–21.
Zhang, A.F., Bian, R.J., Pan, G.X., Cui, L.Q., Hussain, Q., Li, L.Q., Zheng, J.W., Zheng, J.F., Zhang, X.H., Han, X.J., Yu, X.Y., 2012. Effect of biochar amendment on soil quality, crop yield and greenhouse gas emission in a Chinese rice paddy: a field study of 2 consecutive rice growing cycles. Field Crop Res. 127, 153–160.
Zhang, Q., Du, Z.L., Lou, Y., He, X., 2015. A one-year short-term biochar application improved carbon accumulation in large macro aggregate fractions. Catena 127, 26–31.
Zhao, L., Cao, X., Mašek, O., Zimmerman, A., 2013. Heterogeneity of biochar properties as a function of feedstock sources and production temperatures. J. Hazard. Mater. 256–257, 1–9.
Zheng, H., Wang, X., Luo, X., Wang, Z., Xing, B., 2018. Biochar-induced negative carbon mineralization priming effects in a coastal wetland soil: roles of soil aggregation and microbial modulation. Sci. Total Environ. 610, 951–960.